J Mater Sci (2007) 42:6819–6823
DOI 10.1007/s10853-006-1399-3

Combustion synthesis and luminescence characteristic of Eu^{3+}-doped barium stannate nanocrystals

Shumei Wang · Zhongsen Yang · Guangjun Zhou · Mengkai Lu · Yuanyuan Zhou · Haiping Zhang

Received: 1 April 2006 / Accepted: 4 December 2006 / Published online: 26 April 2007

Abstract It is the first time that the undoped and Eu^{3+}-doped barium stannate nanocrystals with definite morphologies are synthesized using a new combustion method. This method offers several attractive advantages such as: currency for any reagents, simple process, surprisingly short calcination time, availability of mass production and good repeatability with low cost. The characteristics of the as-synthesized nanocrystals are described with X-ray diffraction, transmission electron micrograph and luminescence spectrum.

Introduction

Barium stannate ($BaSnO_3$) is a typical compound with a cubic perovskite lattice. The space group is $Pm\bar{3}p$. In the ambient conditions of temperature and oxygen partial pressure it behaves as a pure, n-type semiconductor below 900 °C [1, 2]. These stannates have been investigated in pure as well as in doped forms as potential sensor materials for a host of gases, including CO, HC, H_2, Cl_2, NO_x, and liquefied petroleum gas [3–7]. Due to these noteworthy applications, considerable amount of research have been devoted to the study of synthesis of such materials, such as co-precipitation method [8], low-temperature aqueous syntheses (LTAS) [9], solid-state reaction route [10, 11], self-heat-sustained (SHS) route [12, 13], modified sol–gel route [14], polymerized complex method [15], hydrothermal method [16], chemical precipitation method [17], thermal decomposition [18], and new wet chemical route [19].

All these methods mentioned above use many starting and intermediate chemical components, have many treatment steps, or consume very long time. In this paper, we report a simple $BaSnO_3$ synthesis method, which claims short reaction time, low calcination temperature, simple, mass-produced and has a high level of repeatability. Combustion synthesis which leads to a nearly instantaneous reaction, is an efficient, quick and straightforward method for the preparation of oxide materials, such as aluminates [20–23], chromites [24–27], ferrites [28, 29], manganites [27, 30], titanates [31, 32] etc. It offers several attractive advantages such as process simplification, surprisingly short calcination time, availability of mass production and good repeatability with low cost.

Experiment

All reagents were analytical reagent grade and used without any further purification. The Eu^{3+} ions solution was obtained by dissolving Eu_2O_3 in nitric acid with the concentration of 0.1 mol L^{-1}. Stannic chloride pentahydrate ($SnCl_4{\cdot}5H_2O$) and barium nitrate [$Ba(NO_3)_2$] with Eu^{3+} ions in molar ratios from 3 to 7 mol.% were dissolved in distilled water with the concentration of 0.5 mol L^{-1} for Ba^{2+} and 1 mol L^{-1} for Sn^{4+}, respectively. The mixture of the two solutions had a Ba:Sn molar ratio that corresponded to the stoichiometric (1:1) ratio in $BaSnO_3$ or to different quantities of barium in excess to the stoichiometric amount (Ba:Sn = 1.5:1 and 2:1, respectively) and was added dropwise into ammonia ($NH_3{\cdot}H_2O$)

S. Wang · Z. Yang · G. Zhou · M. Lu (✉) · Y. Zhou · H. Zhang
State Key Laboratory of Crystal Materials, Shandong University, Jinan 250100, China
e-mail: mklu@icm.sdu.edu.cn

aqueous solution with the concentration of 5.2 mol L^{-1} ($V_{NH_2 \cdot H_2O}$:V_{H_2O} = 2:3) under magnetic stirring. The final mixture was alkalescence with a pH value around 9 to ensure the complete reaction of the reagents. The as-synthesized precipitation was filtered and washed with distilled water to remove undesirable anions such as Cl^- and NO_3^-. Then the precipitation was stirred in a solution consisting of ammonium nitrate (NH_4NO_3) and urea [$CO(NH_2)_2$], and heated at 100 °C to minimize the amount of water. Finally, a crucible containing the reagent mixture was placed in an oven kept at 600 °C for 10 min to obtain the Eu^{3+}-doped $BaSnO_3$ nanocrystals. The undoped $BaSnO_3$ nanocrystals were obtained by the same process except for the addition of Eu^{3+} ions.

The crystal phase of the product was determined by X-ray diffraction with CuK_α radiation (RigaKu RIN2200). Transmission electron microscope (TEM) images were taken with a JEM-100CX transmission electron microscope. The photoluminescence properties of the powders were measured with a Hitachi 850 fluoresce spectrometer.

Results and discussion

The X-ray diffraction (XRD) patterns of the as-synthesized nanocrystals are shown in Fig. 1. The XRD signatures of the samples obtained with the initial molar ratio of Ba/Sn less than 2 show a mixture of peaks corresponding to a Sn-rich phase, viz. SnO_2 (JCPDS No: 41-1445), in addition to ones consisting with the intended compound $BaSnO_3$. Nevertheless, that of the sample obtained with the initial molar ratio of Ba/Sn up to 2 only shows the peaks of the phase of $BaSnO_3$ (JCPDS No: 15-0780), indicating that a pure crystal phase of $BaSnO_3$ exists. This phenomenon suggests that barium is provided with volatility during the strong instantaneous reaction. A small amount of the doped ions in the nanocrystals does not change the purity of the nanocrystals since there is one peak related with other compounds including Eu^{3+} ions, as seen from the insert of Fig. 1. It is somewhat surprising to see that there is only one strong shapeliness peak in the XRD pattern of 7 mol.% Eu^{3+}-doped $BaSnO_3$ nanocrystals. This phenomenon indicates that the as-synthesized 7 mol.% Eu^{3+}-doped $BaSnO_3$ nanocrystals tend to be one-dimension crystals.

The synthesis progress of the as-burnt $BaSnO_3$ nanocrystals can be described as follows. During the combustion synthesis, the intermediate product $BaSn(OH)_6$ are used as cation sources of preparation, urea as sacrificial fuel and ammonia nitrate as an additional substance which is able to react with urea, thus increasing the heat released without altering the chemical composition of the final product [27]. For sample preparation, the reactions among the reactants possibly agree with the following equations:

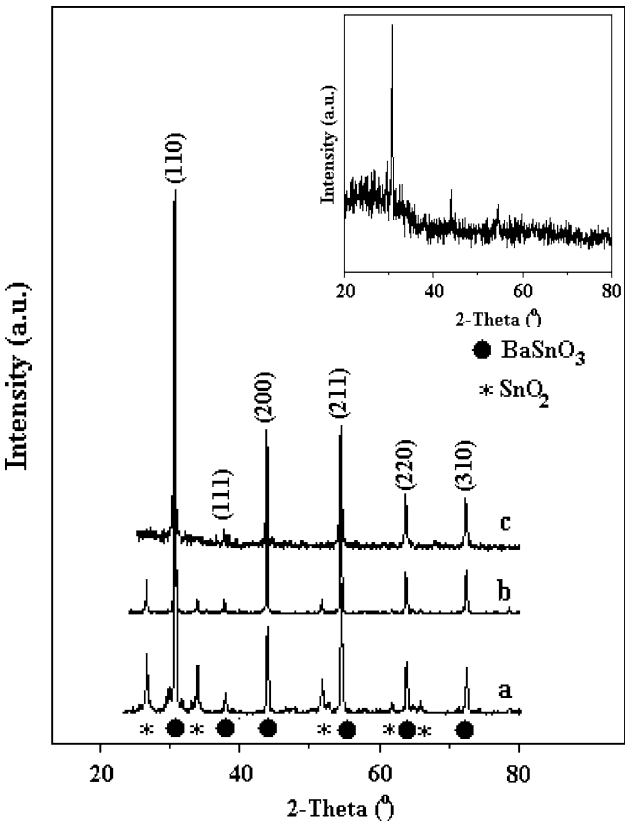

Fig. 1 XRD patterns of the samples synthesized with different ratios of Ba/Sn: (**a**) 1:1, (**b**) 1:1.5, (**c**) 2:1 (Inset: 2:1 doped with 7 mol.% Eu^{3+})

$$Ba(OH)_2 + Sn(OH)_4 \rightarrow BaSn(OH)_6 \quad (1)$$

$$BaSn(OH)_6 + CO(NH_2)_2 \rightarrow BaSnO_3 + CO_2\uparrow + 2NH_3\uparrow + 2H_2O\uparrow + Q_1 \quad (2)$$

$$3NH_4NO_3 + CO(NH_2)_2 \rightarrow CO_2\uparrow + 4N_2\uparrow + 8H_2O\uparrow + Q_2. \quad (3)$$

As stated, Q stands for the heat away from the corresponding exothermic reaction.

Figure 2 presents the transmission electron microscope (TEM) images of the as-synthesized nanocrystals with different magnifications. The morphology of the undoped $BaSnO_3$ nanocrystals is belt. While the 3 mol.% Eu^{3+}-doped $BaSnO_3$ nanocrystals is the mixture of short belt with the size of several tens of nanometers and nanoparticles with the size of several nanometers (Fig. 2b), and the number of the latter is much more than that of the former. When the concentration of the doped ions is up to 5 mol.%, the as-synthesized nanocrystals become quasi-sphere with size under nanoscale (not shown). Then, these super-small particles choose the best orientation to develop to fibers as

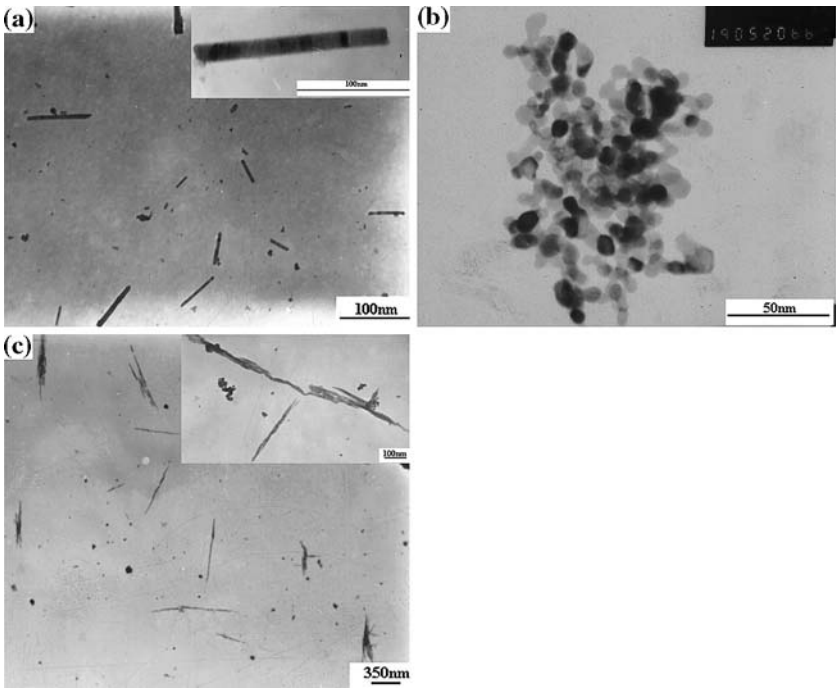

Fig. 2 TEM images of the as-synthesized (**a**) undoped, (**b**) 3 mol.% Eu^{3+}-doped, and (**c**) 7 mol.% Eu^{3+}-doped $BaSnO_3$. (Inset: the corresponding TEM images with the large magnification)

''the leaves of pine'' as seen from Fig. 2c, which accords with the result of XRD very well. It is reasonable to believe that the growth orientation runs along (110) according to what has been shown in XRD patterns.

$BaSnO_3$ is a typical cubic perovskite structure with space group $Pm\bar{3}m$ whereby the morphology of the $BaSnO_3$ compound is cube. But why are the morphologies of the undoped and 7 mol.% Eu^{3+}-doped nanocrystals synthesized by combustion belts and fibers? The explanations are advanced as follows. As mentioned before, there is a possibility to form an intermediate product $BaSn(OH)_6$ because the hydroxide can be synthesized with a small quantity of energy. The morphology with belts accords well with the possible grown morphology of $BaSn(OH)_6$ with the space group $P2_1/n$, which also supplements the formation of $BaSn(OH)_6$. The synthesis progress of undoped $BaSn(OH)_6$ can be displayed as follows:

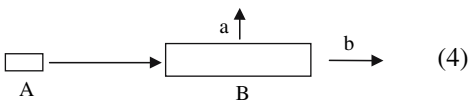

(4)

From the figure above, A is the $BaSn(OH)_6$ nanocrystal synthesized primitively where else B is the grown lamelliform $BaSn(OH)_6$ nanocrystal.

The addition of the Eu^{3+} ions restricts the growth of a and b orientation, while enhances the growth rate of orientation c (a vertical line of a and b). This limiting effect is intensified by the addition of Eu^{3+} ions. This progress is shortened sharply with the addition of the doped ions after the doped concentration level is up to 7 mol.% in this experiment. These progresses are described in Fig. 3. C and D represent the grown $BaSn(OH)_6$ nanocrystals with different $[Eu^{3+}]$. The letter c stands for the vertical growth orientation of a and b. The crucible temperature mushrooms because the combustion progress is an instantaneous exothermic progress just as the depiction of the reaction (2) and (3). At this transitory high temperature, $BaSn(OH)_6$ nanocrystals are dehydrated to form the $BaSnO_3$, and reserve the quondam morphology simultaneously. The similar progress can be seen with the formation of $SrSnO_3$ [33].

The luminescence spectrum of 3 mol.% Eu^{3+}-doped $BaSnO_3$ nanocrystals is displayed in Fig. 4. The most intense transitions observed in the luminescence spectrum originate from the $^5D_0$ level, which is not split by the crystal field ($J = 0$). When excitated at 257 nm, all luminescence lines can correspond to the characteristic transitions from $^5D_0$ to ^7F_J ($J = 0, 1, 2$) states at around 560, 593, and 620 nm, respectively. Although either the hypersensitive $^5D_0 \rightarrow {}^7F_2$ transition (Eu^{3+} site without inversion symmetry), or the magnetic-dipole allowed $^5D_0 \rightarrow {}^7F_1$ transition (Eu^{3+} site

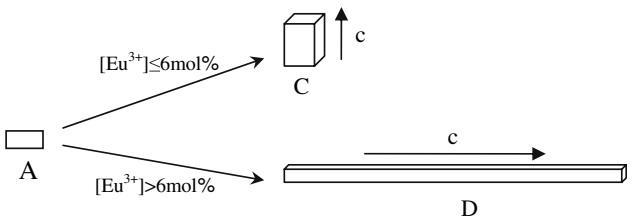

Fig. 3 Description of the morphology changes

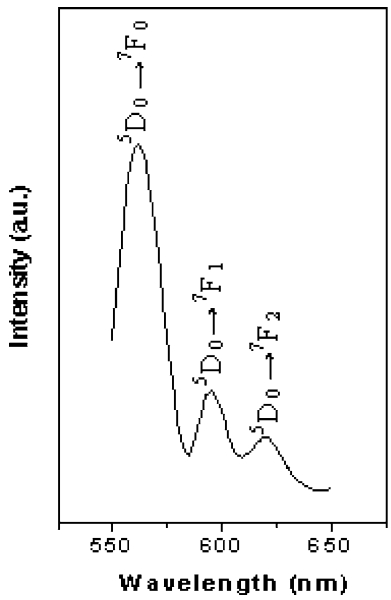

Fig. 4 Emission spectrum of the 3 mol.% Eu^{3+}-doped $BaSnO_3$

with inversion symmetry) can be dominate transition of Eu^{3+} in the $BaSnO_3$ host, no site symmetry is known where the $^5D_0 \rightarrow {}^7F_0$ transition has the highest intensity in the spectrum. On the other hand, the emission intensity of the $^5D_0 \rightarrow {}^7F_0$ transition does not change obviously with the change of the doped concentration (seen from Fig. 5). Therefore, it is unlikely that the yellow emission at 560 nm here is caused by the $^5D_0 \rightarrow {}^7F_0$ transition of Eu^{3+} in a different site. A more likely explanation is that this emission is caused by Eu^{2+} according to the former reports [34, 35]. The fact that Ba^{2+} and Eu^{2+} ions have very close ionic radii explains why Eu^{3+} ions introduced in the Ba^{2+} sites of $BaSnO_3$ are easily reduced to Eu^{2+}, which accords well with the experimental result of Clabau et al. [36]. The emission intensity of Eu^{2+} can hardly change because the luminescence of Eu^{2+} mainly relies on the coordination number, covalency, and crystal field strength at Eu^{2+} site [37]. The existence of

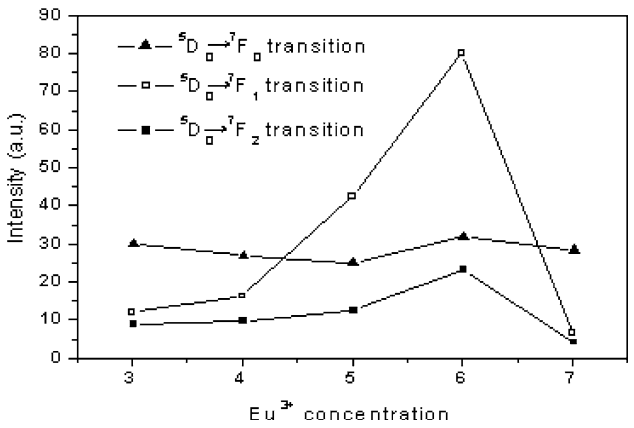

Fig. 5 Emission intensity curves of the as-synthesized nanocrystals

Eu^{3+} emission may be caused by the fact that part of Eu^{2+} is oxidized to Eu^{3+} in ambient atmosphere.

However, there is an interesting phenomenon that with Eu^{3+}-doped nanocrystals especially from 4 to 6 mol.%, the intensity of the peak corresponding to the $^5D_0 \rightarrow {}^7F_1$ transition goes up rapidly and is even higher than the emission intensity of Eu^{2+} ion. The reason may be that there is a possibility of oxygen loss in accordance with the reaction [38]:

$$O_o \rightarrow O_2 + V_o'' + 2e^{\bullet}. \quad (5)$$

On the other hand, the substitution between Eu^{3+} ions and Ba^{2+} ions is of an exchange between the inequi-value ions. Thus, barium loss and abundant positive charges will exist in the as-synthesized doped nanocrystals in accordance with the reaction:

$$Eu_{Ba}^{\times} + E_D \rightarrow Eu_{Ba}^{\bullet} + V_{Ba}'' \quad (6)$$

At room temperature, associations among the forenamed resultants, viz. V_o'', $Eu_{Ba}^{\bullet}$, and V_{Ba}'', will occur, and transfer energy to the $^5D_0 \rightarrow {}^7F_1$ transition, and then enhance its intensity. The decrease of the intensity with the doped concentration up to 7 mol.% is due to the concentration quenching, which contains two types of contributions [39]: (i) energy migration through the lattice; (ii) clusters of activators, which play the role of the killer site.

Conclusions

A strong luminescence emission of Eu^{2+} ions occurs in the doped nanocrystals because Eu^{3+} ions introduced in the Ba^{2+} sites of $BaSnO_3$ are easily reduced to Eu^{2+} with the instantaneous reaction at a low temperature. On the other hand, part of Eu^{2+} ions is oxidized to Eu^{3+} ions. With the increase of the reaction temperature, the crystallinity of the as-synthesized nanocrystals increases, resulting in a great increase in the emission intensity of the nanocrystals. At room temperature, associations among the defects will occur, and transfer energy to the $^5D_0 \rightarrow {}^7F_1$ transition, and then enhance its intensity.

Acknowledgements This work is supported by the funds of excellent state key laboratory (No. 50323006) and the funds awarded by Shandong Province (No. Y2003F08).

References

1. Hines RI, Allan NL (1996) Philos Mag B 73:33
2. Ostrick B (1997) J Am Ceram Soc 80:2153
3. Matsushima S, Teraoka Y, Miura N, Yamazoe N (1988) Jpn J Appl Phys 27:1798
4. Ratna Phani A, Manorama S, Rao VJ (1995) Appl Phys Lett 66:2619

5. Lumpe U, Gerblinger J, Meixner H (1995) Sens Actuators B 97:24
6. Reddy CVG, Manorama SV, Rao VJ, Lobo A, Kulkarni SK (1999) Thin Solid Films 348:261
7. Reddy CVG, Manorama SV, Rao VJ (2001) J Mater Sci 12:137
8. Bao M, Li WD, Zhu P (1993) J Mater Sci 28:6617
9. Leoni M, Buscaglia V, Nanni P, Viviani M (1998) Ceram Trans 88:159
10. Azad A, Hon NC (1998) J Alloys Comp 270:95
11. Azad AM, Shyna LLW, Pang TY, Nee CH (2000) Ceram Int 26:685
12. Upadhyay S, Parkash O, Kumar D (1997) J Mater Sci Lett 16:1330
13. Smith MG, Goodenouth JB, Manthiram A, Taylor RD, Peng W, Kimbal CW (1992) J Solid State Chem 98:181
14. Licheron M, Jouan G, Husson E (1997) J Eur Ceram Soc 17:1453
15. Udawatte CP, Kakihana M, Yoshimura M (1998) Solid State Ionics 108:23
16. Kutty TRN, Vivekanadan R (1987) Mater Res Bull 22:1457
17. Tao S, Gao F, Liu X, Sorensen OT (2000) Sens Actuators B 71:223
18. Reddy CVG, Manorama SV, Rao VJ, Lobo A, Kulkarni SK (1999) Thin Solid Films 348:261
19. Cerda J, Arbiol J, Diaz R, Dezaneau G, Morante JR (2002) Mater Lett 56:131
20. Li F, Hu K, Li J, Zhang D, Chen G (2002) J Nucl Mater 300:82
21. Mimani T (2001) J Alloy Compd 315:123
22. Kwon SW, Park SB, Seo G, Hwang ST (1998) J Nucl Mater 257:172
23. Fumo DA, Morelli MR, Segadaes AM (1996) Mater Res Bull 31:1243
24. Mukasyan AS, Costello C, Sherlock KP, Lafarga D, Varma A (2001) Sep Purif Technol 25:117
25. Yang YJ, Wen TL, Tu H, Wang DQ, Yang J (2000) Solid State Ionics 135:475
26. Kingsley JJ, Pederson LR (1993) Mater Lett 18:89
27. Biamino S, Badini C (2004) J Eur Ceram Soc 24:3021
28. Yue Z, Zhou J, Li L, Zhang H, Gui Z (2000) J Magn Magn Mater 208:55
29. Qi X, Zhou J, Yue Z, Gui Z, Li L (2002) Mater Chem Phys 78:25
30. Caldes MT, Goglio G, Marhic C, Joubert O, Lancin M, Brohan L (2001) Int J Inorg Mater 3:1169
31. Segadases AM, Morelli MR, Kiminami RGA (1998) J Eur Ceram Soc 18:771
32. Jung CH, Park JY, Oh SJ, Park HK, Kim YS, Kim DK, Kim JH (1998) J Nucl Mater 253:203
33. Wang S, Lu M, Zhou G, Zhou Y, Zhang A, Yang Z (in press) J Alloy Compd
34. Li YQ, Delsing ACA, de With G, Hintzen HT (2005) Chem Mater 17:3242
35. Xie RJ, Hirosaki N, Mitomo M, Yamamoto Y, Suehiro T, Sakuma K (2004) J Phys Chem B 108:12027
36. Clabau F, Rocquefelte X, Jobic S, Deniard P, Whangbo MH, Grcia A, Mercier TL (2005) Chem Mater 17:3904
37. Su H, Jia Z, Shi C (2001) Chem Mater 13:3969
38. Gerhardt R (1994) Proc Phys Soc Lond 58:1491
39. Vanderziel JP, Kopf L, Vanuitert LG (1972) Phys Rev B 6:615